ZHU HAI-YAN
DENG JIN-GEN
CHEN ZHEN-GRONG
DONG GUANG
LI JI-RAN
CHEN ZI-JIAN
and
HU LIAN-BO

Hydraulic fracture initiation and propagation of highly deviated well with oriented perforation completion technique

In order to investigate the effect of different perforation angles (the angle between the perforation direction and the maximum horizontal principal stress which is also called the preferred fracture plane (PFP)) on the fracture initiation and propagation during the hydraulic fracturing of highly deviated well, laboratory experiments of the hydraulic fracturing of the BZ25-1 oilfield had been carried out on the basis of non-dimensional similar criteria by using 400mm^3 cement cubes. We built the geometric model of the hydraulic fracturing fractures which considered the influences of the wellbore azimuth (the angle between the wellbore axis and the PFP), the perforation angle and the well deviation. The results showed that: the perforations in the PFP produce plane fracture; the fractures initiate from the perforations at the upper side of the well hole and then turn to the PFP when the perforation angle is 45°; when the well deviation angle and the perforation angle are both larger than 45°, the fracture initiates difficultly from the perforations at the lower side of the well hole, and multi-fractures easily initiate; when the perforation angle is 90°, multi-fractures initiate, such as twisting fracture, plane fracture, horizontal fracture and T-shape fracture, in addition, the fracture cannot initiate from the perforation tunnels; the larger the well deviation angle is, the easier is the multi-fractures initiation. Moreover, it is easier to result in micro-annulus which makes the fractures more complicated during the hydraulic fracturing of highly deviated well when the perforation angle is not along with the PFP. Oriented perforating technology should be applied in highly deviated well to obtain the big single plane fracture.

Keyword: *Oriented perforating; highly deviated well; hydraulic fracturing; fracture initiation; fracture propagation.*

Messrs. Zhu Hai-yan, Deng Jin-gen, Chen Zhen-grong, Dong Guang, Li Ji-ran, Chen Zi-jian, Hu Lian-bo, State Key Laboratory of Petroleum Resource and Prospecting (China University of Petroleum, Beijing), Beijing 102249, China. E-mail: zhuhaiyan040129@163.com

1. Introduction

Hydraulic fracturing is an important technical measure in well production increment and intensified injection of the injection wells. It could improve the seepage field of the rocks near the bottom hole, make the oil and gas connect to the bottom hole and improve the flow condition of the oil and gas, so as to increase the well production. Field practices indicate that most hydraulic fracturing works are operated in cased well with perforating completion technique, the perforation tunnels is the flow path of the fracturing fluid between the hydraulic fractures and well hole (Abass [1]; Mahrer [2]). Many scholars (EI Rabaa [3]; King [4]; Behrmaan and Elbel [5]; Hallam and Last [6]; Pearson et al [7]; Daneshy [8]) have proposed that the hydraulic fracturing could produce a large plane fracture when the perforations are consistent with PFP, which means that the perforation angle is 180° or 0°. When there is a random angle between the perforations and PFP, the fracture geometry would be complicated; the greater the angle is, the higher is the fracture initiation pressure, the lower is the probability of the fracture initiation from the perforation tunnels, the more is the complicated fracture geometry.

Due to the difficulty indirect observation of the fracture initiation and propagation, the indirect analysis is often by means of numerical model based on various assumptions and simplified conditions (PKN (Nordgren [9]), GDK (Khristianovic and Zheltov [10]; Geertsma and de Klerk [11]), radial Penny model (Sneddon and Elliot [12]), PL3D (Clifton and Abou-Sayed [13]; Siebrits and Peirce [14]), P3D (Mack and Warpinski [15]), etc.). Hydraulic fracturing experiment which considers the formation condition is an important mean of understanding fracture initiation and propagation mechanism. It could monitor the progress of fracture initiation and propagation and observe the fractures directly. Table 1 enumerates the test parameters of typical laboratory hydraulic fracturing experiments since the 1970s. We can find that the studies about the initiation and propagation mechanism of the hydraulic fractures are mostly proposed between the 1970s and 1990s. The cement and the mixture of cement and sand are dominant as the test examples. Rock sample size which simulated the vertical and horizontal well is mainly 152*152*254 mm and the deviated well is mainly 300 mm^3. Meanwhile, Crosby et al. [16] used the 400 mm^3 sample for the simulation of horizontal well hydraulic fracturing, and Ahmed et al. [17] used 1m^3 stratified rock block for the vertical well. The perforating phase angles of the vertical and horizontal wells are mainly 0° and 180°, and the fracture initiation and propagation mechanism under different well deviation angles and azimuth angles are studied. Among these studies, van de Ketterij and de Pater [18] studied the fracture initiation and propagation mechanism for the perforation angle of 0°, 90° and 180° under 60° well azimuth and 45° well deviation. Deng et al.19, 20 simulated the fracture initiation and propagation mechanism of deviated well with oriented perforating completion technique at 30° well deviation. We can see that the hydraulic fracturing experiments of deviated well use 300mm^3 rock samples, and their boundary effects are serious; the systematic researches on hydraulic fracturing under different well azimuth angles and perforation angles for highly deviated well are lacked. In this paper, laboratory hydraulic fracturing experiments using 400 mm^3 rock samples are carried out to study the influences of oriented perforating on the fracture initiation and propagation of highly deviated well under different well deviation and perforation angles, which could find out the fracture initiation and fracture propagation mechanism of highly deviated well, and provide the theoretical guidance for hydraulic fracturing in highly deviated well.

TABLE 1 TEST PARAMETERS IN THE HYDRAULIC FRACTURING EXPERIMENTS

Parameters	Daneshy	Daneshy	Ahmed et al.	Rabaa	Hallam and Last	Kim and Abass	Abass	Weijers	Brumley and Abass	Van de Ketterij and de Pater	Deng et al.	Jiang et al.
Time	1972	1973	1983	1989	1991	1991	1992	1992	1996	1997	2003/2008	2009
Sample ingredients	Water, cement	Limestone or cement	Cement	Cement	Cement, silica sand powder	Cement	Cement	Cement and fine sand	Cement	Cement and fine sand	Cement and sand	Cement and fine sand
Mix ratio of water to cement or sand	0.35	0.35		0.35	9/1/3	0.32	0.32	1/0.43	0.32	27/23	3/1	1/1
Size mm	150*150*250	150*150*250	1000^3	150*300*450	300^3	150*150*250	150*150*250	300^3	150*150*250	300^3	300^3	300^3
Borehole diameter mm	8	8	3.2	8	6.4	19	19	20	76.2	20	20	20
Casing inner diameter mm	6	Open hole		Open hole	4.8	16	16	19.5	Open hole	8	8	15
Perforations/per rank	10,6,5,3,2,1		15			7	7	1?9		9	2-4	3
Perforation diameter mm	3.2		1		0.4	2.4	2.4	3		3	4	2
Perforation length mm	3.2				7	20.8	20.8	25		25	20	30
Perforation space mm	20-30				9.4	10.4	10.4	12.5		12.5/50		
σ_v MPa	7	7	13.8	51.7	14	20.7	20.7	23	20.7	23	13	15
σ_H MPa	5.5	5.5	13.1	50.3	14	17.2	17.2	12.1	17.2	12.1-19.4	11	4-6
σ_h MPa	3.5	3.5	8.3	38.5	4.8	9.7	9.7	9.7	9.7	9.7	9	1
Inclination	Vertical	8, 16, 24	Vertical	Horizontal	0, 10, 20, 30	Horizontal	Horizontal	45/49	0,22.5, 45,67.5, 90	49	0,30	Vertical
Azimuth	30,60,90	0-75°		0,15,35, 55,75,90	0,10,20, 30,90	0,15,35, 55,75,90	0,15,30,34,45, 60,67.5, 90	30,60	0,22.5, 45, 67.5, 90	60	0,30,45,90	0,15,30, 45,60,75
Phase azimuth	0,180, spiral	0,180			180	180	180	0,180		0,90,180	180	180
Test liquid			Fracturing liquid	10# heavy engine oil	Lubricating oil	30# heavy oil	30# engine oil	100# oil	Fracturing liquid	Fracturing liquid	heavy hydraulic fluid	Guanidine gum liquid
Viscosity Pa.s			0.030-0.3	0.36-0.58	6.5	0.36-0.58	0.36-0.58	0.3	1.3	0.1/0.5	0.1	0.073
Injection rate cm^3/min	136.2	136.2, 1020-1380	204-582	84-333	10	40	30	0.2-1	10	0.088-0.44		0.126

2. Design of hydraulic fracturing laboratory experiment of oriented perforation

2.1 Parameters of oriented perforating hydraulic fracturing experiment

The size limitation of the laboratory experiment equipment makes it impossible to simulate the full-scale test of hydraulic fracturing, so the numerical scaling for experimental rock, perforation tunnel, injection rate and the fracture fluid property is necessary. Pater et al. [21] introduced a scale model for the laboratory experiment based on the theoretical analysis and the laboratory experiment. The critical factors that decide the experiment is the in-situ stresses, high viscosity fluid, and low injection rate. They also proved that the hydraulic fracture propagation driven by high pressure fluid is a kind of linear elastic fracture in the laboratory experiments. Using the equation analysis method of the similarity theory, Pang [22] deduced the similar criteria of the hydraulic fracturing simulation experiment. The experiment should consider the in-situ stresses, the rock samples with lower fracture toughness and lower permeability, and fracturing fluid with higher viscosity and minimal injection displacement. Considering the fracture fluid as the Newtonian fluid, Bunger et al. [23] concluded that the fracture propagation is related to three timescales which are fluid lag, fluid viscosity and fluid leak-off. Based on these conditions, they introduced the laboratory experiment design scale for the penny-shaped fracture. These two scales are based on the assumption that the fracture propagation is in the two-dimensional plane, which is not feasible for the experiment of hydraulic fracturing in deviated well with oriented perforation completion technique. So, a three-dimensional parameters scale model should be applied for the fracture propagation with oriented perforation completion technique. Liu et al. [24] introduced the similarity principle of the laboratory experiment by the pseudo three-dimensional model of hydraulic fracturing established by Clitton and Abou-Sayed [25] as the control equation of fracture propagation. For the parameters of the well A1 in the BZ25-1 oilfield, the experimental parameters obtained by the similarity principle are listed in Table 2.

Table 2 Basic experimental parameters

Parameter	Experimental parameters	Field parameter
Wellbore size (mm)	18	177.8 (7 in)
Perforation interval (mm)	20	200
Perforation row	3	3
Perforation diameter (mm)	2	>=9
Perforation length (mm)	60	>= 300
Injection rate (cm^3/min)	0.1	2000000
Viscosity of fracture fluid (Pa·s)	0.5	0.04-0.6

2.2 Experimental device of oriented perforating hydraulic fracturing experiment

The hydraulic fracturing experiment was tested on the 400 mm cubic tri-axial hydraulic fracturing test equipment designed by the rock mechanics laboratory of China University of Petroleum (Beijing) (Fig.1). The horizontal principal stresses are generated by the four cranes around the sample and the vertical stress is loaded by the crane blow the sample. The rigid load is imposed to the 400 mm^3 rock by the flat jack which is supported by the multi-channel constant voltage source for the hydraulic pressure, and the pressure of every channel whose maximum is 60 MPa could be controlled respectively. Using the MTS servo booster pump, the high-pressure liquid is pumped into the simulation borehole in this experiment. MTS booster pump has a programme controller which can either inject liquid at a constant displacement or work by the pre-set infusion procedures. The pressure is observed and recorded by MTS data acquisition system during the experiment. More detail information about the schematic diagram of tri-axial hydraulic fracturing test system can be seen from the paper published by Zhou et al.26.

Fig.1 400 mm^3 true tri-axial hydraulic fracturing test equipment

2.3 The scheme design of oriented perforating hydraulic fracturing experiment

We simulate different perforation angles and well azimuth angles for 0°, 30°, 45° and 60° well deviation angles, respectively (Table 3). Fig.2 illustrates the rock sample size and the location of the perforation tunnels. We use the concrete made by combination of cement and fine-sand with the proportion of 1:1 for the experiment. The *E* of the concrete is 8.4 GPa, the *v* is 0.23, the tensile strength is 3.1 MPa, the UCS is 29.2 MPa, the permeability is 0.2 mD, and the porosity is 2.32%. A special mold is designed to make a 400mm^3 rock sample, the mold is consisted of one bottom plate and four

TABLE 3 EXPERIMENT SCHEMES

	Displacement L/min	Deviation°	Azimuth°	Perforation angle°	Perforation length mm	Side distance mm	Top distance mm	Bottom distance mm
1	0.126	0	0	0	0	195	190	170
2	0.126	45	0	0	60	110	142	145
3	0.126	45	0	45	60	110	142	145
4	0.126	45	0	90	60	110	142	145
5	0.126	45	45	0	60	110	142	145
6	0.126	45	45	45	60	110	142	145
7	0.126	45	45	90	60	110	142	145
8	0.126	45	90	0	60	110	142	145
9	0.126	45	90	45	60	110	142	145
10	0.126	45	90	90	60	110	142	145
11	0.126	30	45	45	60	113	157	148
12	0.126	60	45	45	60	113	128	148
13	0.126	45	0	0	0	153	184	188

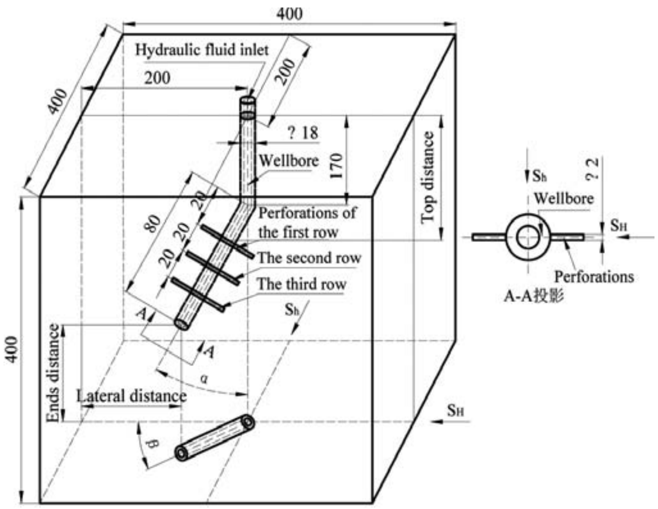

Fig.2 Size of the sample and the perforation location

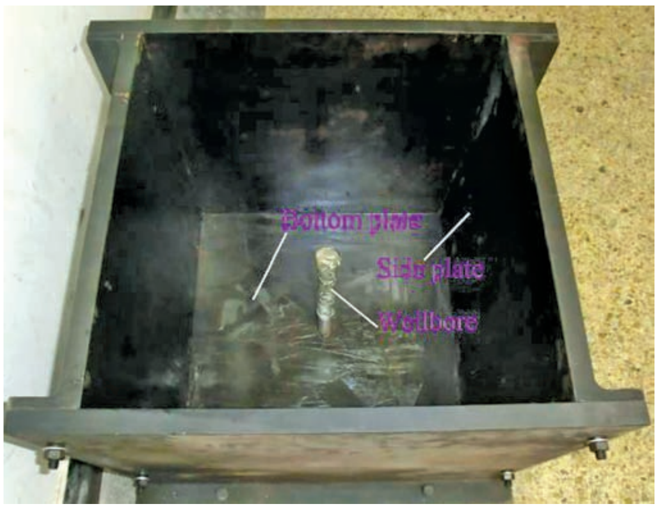

Fig.3 Rock sample mold and simulated wellbore

side plates, as shown in Fig.3. In order to prepare the sample, we put four side plates stand on the bottom plate and connect them with each other by eight bolts (the flange edge on the bottom plate and the datum line on the side plate are used for the location of the side plate). Coat the lubricant over the inside of the cabinet and insert the simulated wellbore inversely into the sink hole on the bottom plate. The simulated wellbore is a steel pipe whose outer diameter is 18 mm, inner diameter is 8 mm and it is used to simulate the borehole. Holes of 2 mm diameter are drilled at 20 mm away from the bottom of the steel pipe, and some plastic pipes which simulate as the 60 mm pre-set perforation tunnels are inserted into these holes. After that, pour the concrete which is made from the 425# building cement, fine sand and water into the cabinet and cover the top plate. Remove it out when it solidified.

3. The experimental results

We carried out the hydraulic fracturing experiment of the open hole deviated well with well deviation of 45° and well azimuth of 0°. The results show that: there are four fractures around the borehole and two of them are linked-up with each other; a big plane fracture initiates along the lower side of the borehole and connects to the upper surface fracture; there are two smaller fractures at the upper side of the borehole (Fig.4[a]), one is in the σ_H direction and it connects to the big plane fracture at the upper side of the borehole, another is in the σ_h direction and it connects to the above fracture in σ_H direction, the big plane fracture at the lower side of the borehole and the surface fracture at the upper side of the borehole (Fig.4[b]); the branch fractures and secondary fractures are initiated and the fracture surfaces are rough. The results are consistent with the experiment results done by Brumley and Abass [27] which further confirms the reliability of the simulation. The fracture initiation pressure is 25.9 MPa and the fracture propagation pressure is 20.8 MPa in this

TABLE 4 FRACTURE INITIATION AND PROPAGATION PRESSURE

	Well deviation°	Well azimuth°	Perforation angle°	Initiation pressure MPa	Propagation pressure MPa	Forecasting pressure MPa
2	45	0	0	24	18.5	58.80
3	45	0	45	25.6	20.2	62.72
4	45	0	90	27	20.5	71.55
5	45	45	0	24.5	18.7	60.03
6	45	45	45	26.4	19.6	64.68
7	45	45	90	27.2	21.4	72.08
8	45	90	0	23.6	18.6	57.82
9	45	90	45	26.8	20.9	65.66
10	45	90	90	27.3	20.9	72.35
11	30	45	45	22.2	18.4	58.83
12	60	45	45	28.2	22.4	74.73

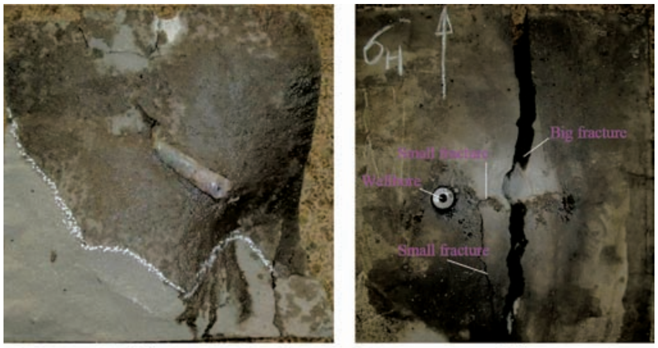

(a) (b)

Fig.4 Fracture propagation of a open hole well with 45°perforation angle and 45°deviation angle

experiment. Based on similar criteria, the fracture initiation pressure of this kind of well in the field is 63.5 MPa. The error is 2.3% when compared to the analytic solution which is about 65 MPa.

3.1 INFLUENCES OF THE WELL AZIMUTH, WELL DEVIATION, AND PERFORATION ANGLE ON THE FRACTURE INITIATION AND PROPAGATION

The initiation pressure, propagation pressure of the sample and the forecasting pressure of the formation are illustrated in Table 4. When the well deviation is 45° and the well azimuth angles are the same, the fracture initiation pressure increases with the increasing of the perforation angle (Fig.5). When the perforation angles are 45° and 90°, the fracture initiation pressure and propagation pressure increase with the well azimuth angles. When the perforation angle is 0°, the fracture initiation pressure increases at first

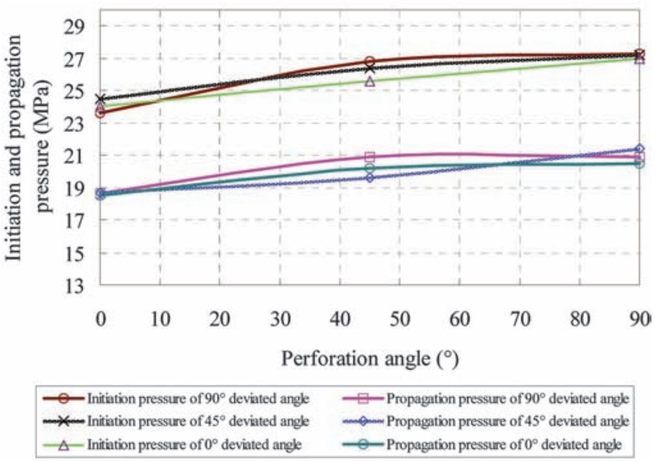

Fig.5 Perforation angles versus initiation and propagation pressure

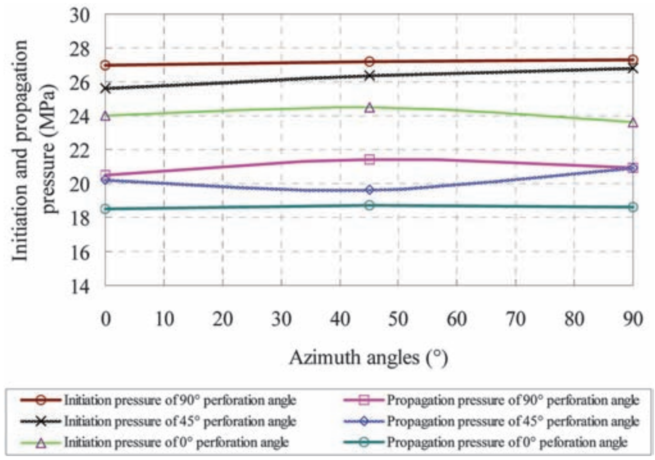

Fig.6 Azimuth angles versus initiation and propagation pressure

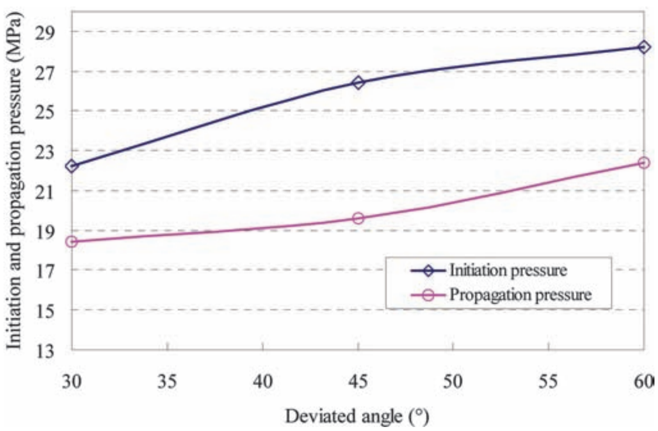

Fig.7 Deviated angles versus initiation and propagation pressure

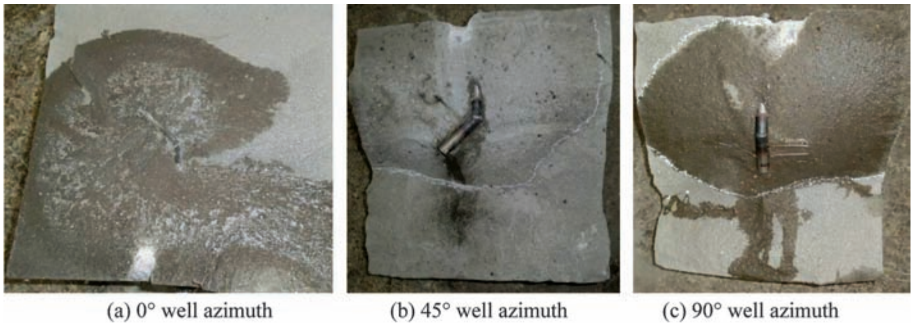

Fig.8 Fracture propagation with 0° perforation angle

(2) 45° perforation angle

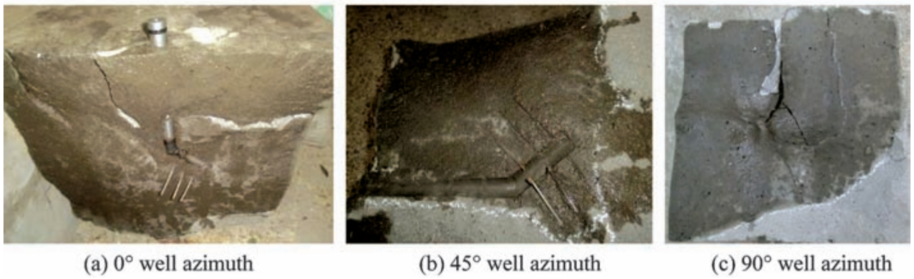

Fig.9 Fracture propagation with 45° perforation angle

then decreases with the well azimuth angle increasing, the maximum value appears when the well azimuth is 45° and the minimum value appears when the azimuth is 0° or 90°; the propagation pressure increases with the increasing of the well azimuth (Fig.6). Fig.7 illustrates that the fracture initiation and propagation pressure increase rapidly with the increasing of the deviation.

3.2 Influence of the perforation angle on the fracture initiation and propagation

(1) 0° perforation angle (oriented perforation)

The fractures all initiate along the perforation tunnels in the PFP. When the well azimuth is 0°, a large-plane fracture is generated (Fig.8a); if the well azimuth is 45°, the fracture initiates in the PFP and propagates mainly at the upper part of the wellbore (Fig.8b). The surface of the fracture is rough and secondary fracture occurred. When the well azimuth is 90°, a smooth plane fracture initiates (Fig.8c). The fractures with different well azimuth angle did not initiate at other point, which suggests that there is no micro-annulus developed during the hydraulic fracturing. What should be noticed is that when the perforation is at the direction of well azimuth 45°, though the fracture initiates at both sides of the wellbore, it does not propagate further at the lower side of the wellbore, because the fracture at the upper side of the wellbore reaches the rock face firstly and then the pressure in the fracture decreases rapidly to the point that the lower facture can not propagate any further.

The geometric shapes of the fractures are very complicated, there are plane fractures, turning fractures, parallel fractures, secondary fractures and discontinuous fractures etc. When the well azimuth is 0°, the fractures initiate along the perforations at the lower side, turn to the PFP and form a spacing surface fracture; micro-annulus exists and the fracturing liquid runs around the borehole axis about 45°, then form a big plane fracture; at the same time there are three secondary fractures (Fig.9(a)). When the well azimuth is 45°, the fractures initiate along the perforations at the upper side, turn to the PFP and form a turning surface fracture; the fractures in the lower side initiate along the perforations but terminate quickly (Fig.9(b)). When the azimuth is 90° (Fig.9(c)) the fractures initiate along the perforations at the upper side, turn to the PFP and form surface fractures; though the perforations in the lower side initiate but the fractures disappeared very quickly; there is a micro-annulus which propagate lower along the PFP and form plane fractures; there are discontinuous phonemes and two secondary fractures at the upper side of the borehole.

There are T-shaped fracture, horizontal fracture, turning fracture, branch fracture etc. As illustrated in Fig.10(a), the perforations in the first row initiate when the well azimuth is 0°; when they twist to the PFP, the rocks around the borehole initiate in the plane which is perpendicular to the perforations because of the micro-annulus and propagate rapidly, at last the twisting fractures in the both sides of the borehole connect and form a big horizontal fracture, with the growth of this fracture, there appeared a horizontal surface whose middle is depressed and the outermost of the fractures upturn to the PFP; at the same time there are four branch fractures in the direction of σ_H; the fractures do not initiate in the second and third row perforations. The Fig.10(b) illustrates that when the well azimuth is 45°, the fracture geometry is the same as 0° well azimuth, the fracture is a horizontal surface whose middle is depressed and the dip angle between the surface and the horizontal plane is 45°, so the middle part fracture is parallel to the simulated borehole axis; the fracture surface is rough and there are some turning fractures in the direction of σ_H; only the perforations in the third row at the upper side initiate; the fracture surface is very rough and five secondary fractures exist. Fig.10(c) illustrates that when the well azimuth is 90°, there is a fracture at one side of the direction of σ_H; the fractures initiate along the perforations at the upper side, the adjacent fractures connect and form an initial fracture surface, then this surface turn to the σ_H and propagate and form a raised surface; there is no fracture from the perforations

(a) 0° well azimuth (b) 45° well azimuth (c) 90° well azimuth

Fig.10 Fracture propagation with 90° perforation angle

in the lower side of the borehole; there are some fractures near to the upper side of the borehole.

The results showed that: when the perforation angle is 0°, there exists a large plane fracture; when the perforation angle is not 0°, the geometrical shapes of the fractures are very complicated; when the perforation angles are the same, the bigger the well azimuth angle is, the much more complicated are the geometrical shapes of the fractures; when the well azimuth angles are the same, it is difficult for the fractures to initiate along the perforations and the geometrical shapes are more complicated with the perforation angle increasing.

3.3 Influence of the well deviation angle on the fracture initiation and propagation

When the well azimuth and the perforation angle are both 45°, we consider the fracturing conditions that the well deviation angle are respectively 30°, 45° and 60°. Fig.11(a) illustrates that when the well deviation is 30°, the fractures initiate along the perforations, turn to the PFP and form a surface fracture with two nearly symmetric wings; there are discontinuous fractures. Fig.11(b) illustrates that when the well deviation is 45°, turning surface fractures appear at the upper side of the borehole; though the fractures in the lower side of the borehole initiate but did not propagate any further. In conclusion, the fracture geometrical shape is more complicated; the fracture initiation and propagation pressure are larger when the well deviation angle increases.

3.4 Influence of the well azimuth angle on the fracture initiation and propagation

When the well azimuth is certain, the fracture geometrical shapes become more complicated as the perforation angle increases. No matter how about the well azimuth angle changes, this relationship remains the same. Under the same well azimuth angle, when the perforation angle changed from 0° to 90°, the fractures would change from plane fracture to turning fracture, multi-fractures and horizontal fracture in the end. The well azimuth has a large influence on the fracture surface roughness, the secondary fracture and the continuity, but has little influence on the fracture geometrical shape.

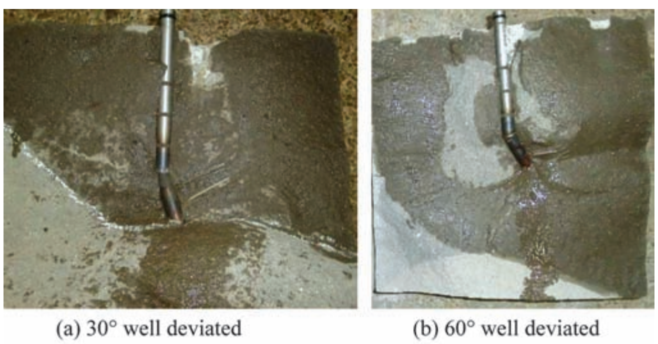

(a) 30° well deviated (b) 60° well deviated

Fig.11 Fracture propagation versus different deviated angle

4. Discussions

4.1 In-situ stress difference

The ratio of the horizontal stresses in this simulation (the maximum horizontal stress/the minimum horizontal stress) is 1.23. According to the experiment results, the fractures include double wings fracture, turning fracture, multi-fracture, twisting fracture and horizontal fracture. Doe and Boyce [28] carried out a laboratory hydraulic fracturing experiment on salt. They studied systematically the fracture geometrical shape when the horizontal stresses ratio changes from 1 to 2, and found that: when the horizontal stresses ratio is more than 1.5, the fracture is a single plane fracture; when the horizontal stresses ratio changes from 1.5 to 1, the branched fractures and multi-fractures appear, the fractures become much more complicated when the ratio decreases. Beach [29] and Daneshy [30] et al. conclude the same results later. Behrmann [5] done the hydraulic fracturing experiments of the vertical and horizontal well under the ratio 1.22, they also found the performance of the double wings fracture, multi-fracture and near-wellbore fracture etc. The results of this paper for the highly deviated well also showed that the fractures become much more complicated when the horizontal stresses ratio decreases. The ratio of the maximum horizontal stress and the vertical stress is 1.07, which means the maximum horizontal stress is approximately equal to the vertical stress. This particular stress conditions may easily create the horizontal fracture which is observed in our experiments.

4.2 Micro-annulus

There is rarely micro-annulus when the perforation angle is 0° such as the sample 2#, 5# and 8#. However, when the perforation angle is 45° or 90°, there would appear micro-annulus no matter what the well deviation and well azimuth are. The results further verify the accuracy of the current fracture initiation model of the spiral perforating completion technique. So far, the petroleum engineers and scholars consider that a micro-annulus exits between the casing and the cement sheath or the cement sheath and the formation during the hydraulic fracturing. The fracturing fluid firstly flows into the micro-annulus and the perforation tunnels; then the fractures initiate at the point where the fracture initiation pressure are the lowest around the wellbore surface, which means that the hydraulic fractures do not always initiate in the perforation tunnels. This fracture initiation phenomenon is obtained by our experiments. Considering the existence of the micro-annulus and neglecting the effect of the casing on the stress distribution around the wellbore, the current model of the fracture initiation pressure is calculated (Yew [31]; Yew [32]; Soliman [33,34]; Hossain [35,36]; Crosby [16,37]; Biao [38]; Fallahzadeh [39,40]; Ketterij [18,41]; Weng [42]; Luo [43]; Abass [1]; Chen [44]; Deng [45]; Osorio [46]). However, if the perforation direction is along with the PFP, the hydraulic fracture will grow in the perforation tunnels and the micro-annulus will never emerge. So, the hydraulic fracturing initiation pressure using orientated perforating technique does not conform to this practical situation. So, the stress distribution around the wellbore should consider the influence of the casing for the fracture initiation model with orientated perforating completion technique. In order to obtain a single big plane fracture, the orientated perforating completion technique is suggested.

4.3 Discontinuity of the fracture

Hallam and Last [47] carried out hydraulic fracturing experiments with perforating completion technique of the moderate deviated well. When the well deviation is less than 10°, the fracture surface is smooth no matter what the well azimuth is; when the well deviation is more than 20°, the well azimuth of producing smooth fracture surface can be expressed as:

$$\tan\beta = \frac{(\sin^2\beta\sin^2\alpha + \cos^2\beta)^{0.5}}{\sin\beta\cos\alpha} \quad \text{... (1)}$$

We can find when the well deviation is 45° and well azimuth is more than 13°, there is discontinuous fracture. According to the results of this paper, when the deviation is 45° and the well azimuth is 90°, the fracture surface is still smooth. It cannot be accepted that Hallam and Last [6] used the well deviation and well azimuth to judge whether there is continuous fracture. Weng [42] used the well deviation, well azimuth, in-situ stress differentiation and the static pressure in the fracture to judge whether the hydraulic fracturing would produce the continuous fracture, they proposed the following equations of the critical angle of producing discontinuous fracture:

$$\sin\gamma_{crit} = 0.57\,(\Delta\sigma/P_{net})^{-0.72} \quad \text{... (2)}$$

$$\gamma < \gamma_{crit} \quad \text{... (3)}$$

When the fracture initiation angle is less than the critical angel, the fracture is continuous. According to our experiments, when the deviation is 45° and the well azimuth is 90°, the initiation angle γ is zero and always less than or equal to γ_{crit}, so there is no discontinuous fractures.

4.4 The spacing and length of perforation tunnel

In order to avoid the discontinuous fracture, Hallam and Last [6] proposed the perforation spacing should be less than 330mm, and the length is about 100-150mm. Stadulis [47] suggested that 0° perforation angle and less than 304 mm perforation spacing can produce a big plane fracture. In our experiment, the perforation parameters are taken as the perforation spacing of 200 mm and length of 600 mm. No matter what the well deviation is, there exists a plane fracture when the perforation angle coincides with the PFP. So the perforation parameters can be used in the hydraulic fracturing of BZ25-1 oilfield.

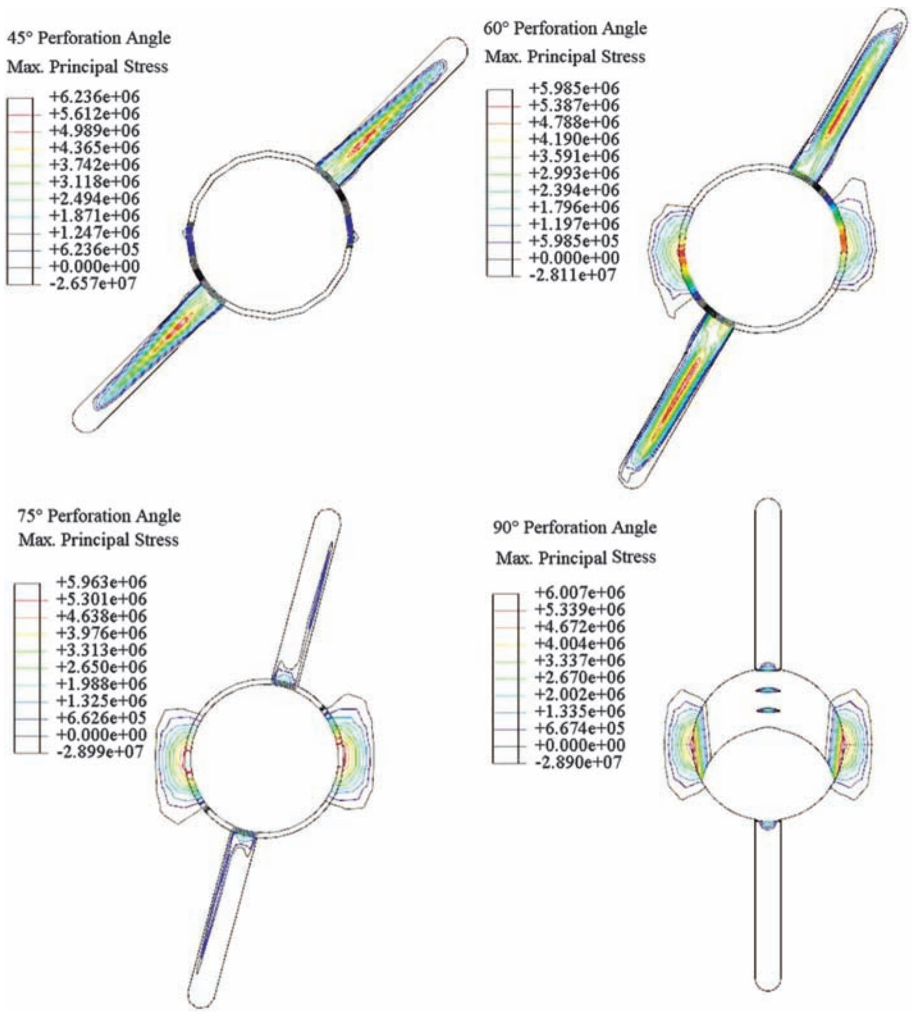

Fig.12 The max. principal stress with different perforation angles

4.5 Fracture geometrical shapes of different well azimuth angles and perforation angles

Ketterij and De Pater18,41 carried out the hydraulic fracturing experiments for the deviated well with well deviation of 49°, well azimuth of 60° and perforation angle of 0°, 90° and 180°. They found that the perforation angle of 180° is the most beneficial to the series connection of the fractures and the perforation angle of 90° is converse. Those are consistent with the results. In order to further understand the fracture initiation mechanism, considering the influences of the fluid penetration, the excavation processes of the wellbore and the perforation tunnels, the seepage coupled deformation finite element model (FEM) of the highly deviated well with perforating completion technique is established using the tensile strength failure criterion. Substituting the parameters of the well A1 in the BZ25-1 oil field to the FEM, we calculate the model when the well deviation angle is 45°, the well azimuth angle is 0°, and the perforation angle are 45°, 60°, 75° and 90° (Fig.12). The maximum principal stress with each perforation angle is shown as the colourful isolines. When the tensile strength of the formation rock is zero, the places of the coloruful isolines are the potential initiation points, that is to say when the perforation angle is larger than 45°, the fracture will initiate on the wellbore face in the PFP (the horizontal direction), which is the same as the experiments.

5. Conclusions

The error between the formation initiation pressure based on the experimental results and the analytical solution is less than 2.3%, so the results can be used in predicting the fracture initiation and propagation in the hydraulic fracturing of BZ25-1 oilfield. Meanwhile, when the perforation spacing is chosen as 200 mm, the length is designed as 600mm, and the perforation angle is zero in BZ25-1 oilfield, the fractures can form a single plane fracture. So these operation parameters are suggested for the hydraulic fracturing of this oilfield.

The initiation and propagation pressures increase with the increasing of the well deviation, well azimuth and perforation angle. When the well deviation and well azimuth are certain, the perforation angle should be set as 0° (oriented perforation), so as to decrease the fracture initiation and propagation pressure.

When the perforations are not in the PFP, the geometrical shapes of the hydraulic fractures of the highly deviated well are very complicated; the fractures are the turning fracture, twisting fracture, parallel fracture, horizontal fracture, T-shape fracture etc. The fractures are more complicated when the well deviation and perforation angle increase. So during the hydraulic fracturing of the highly deviated well, in order to obtain a big plane fracture, the perforation should be in the PFP.

The well azimuth angles affect the roughness of the fracture surface, the creation of the secondary fractures and the fracture continuity rather than the fracture geometrical shape. In addition, they would increase the fracture initiation and propagation pressure.

When the perforation angle is 45° and 90°, there would appear a micro-annulus around the borehole. The micro-annulus leads to complicated fractures, breaks the cement sheath and decreases the quality of well cementation. So, it is very important to avoid the existence of the micro-annulus. When the perforations are in the PFP, the micro-annulus may not exist, the fracture initiation pressure calculated by the stress distribution around the open hole well may not correct, it is necessary to consider the influence of the casing on the stress distribution around the wellbore.

Acknowledgments

This work was supported by the Key Program of National Natural Science Foundation of China (51134004), and the National Science and Technology Major Project of the Ministry of Science and Technology of China (No. 2011ZX05024-003-02).

References

1. Abass, H.H., Brumley, J.L., Venditto, J.J. (1994): Oriented perforations - a rock mechanics view. Annual Technical Conference and Exhibition, New Orleans, Louisiana. 25-28 September.
2. Mahrer K.D., Aud W.W., Hansen J.T. (1996): Far-Field Hydraulic Fracture Geometry: A Changing Paradigm. Annual Technical Conference and Exhibition, Denver, Colorado, USA. 6-9 October.
3. EI Rabaa, W. (1989): Experimental study of hydraulic fracture geometry initiated from horizontal wells. Annual Technical Conference and Exhibition, San Antonio, Texas. 8-11 October.
4. King, G.E. (1989): Perforating the horizontal well. *J. Pet. Technol.* 41(7), 671-672.
5. Behrmann, L.A., Elbel, J.L. (1991): Effect of perforations on fracture initiation. *J. Pet. Technol.* 43(5), 608-615.
6. Hallam, S.D., Last, N.C. (1991): Geometry of hydraulic fractures from modestly deviated wellbore. *J. Pet. Technol.* 43(6), 742-748.
7. Pearson, C.M., Bond, A.J., Eck, M.E., Schmldt, J.H. (1992): Results of stress oriented and aligned perforating in fracturing deviated wells. *J. Pet. Technol.* 44(1), 10-18.
8. Daneshy, A.A. (1973): A study of inclined hydraulic fractures. *SPE Journal*. 13(2), 61-68.
9. Nordgren, R.P. (1972): Propagation of a Vertical Hydraulic Fracture. *SPE Journal*. 12(4), 306-314.
10. Khristianovic, S.A., Zheltov, Y.P. (1955): Formation of vertical fractures by means of highly viscous liquid.

In: Proceedings of the fourth world petroleum congress, Rome , Italy. 6-15 June.

11. Geertsma, J., de Klerk, F. (1969): A rapid method of predicting width and extent of hydraulically induced fractures. *J. Pet. Technol*. 21(12), 1571-1581.

12. Sneddon, IN., Elliot, HA. (1946): The opening of a Griffith crack under internal pressure. *Q. Appl. Math*. 4(3), 262-267.

13. Clifton, R.J., Abou-Sayed, A.S. (1981): A variational approach to the prediction of the three-dimensional geometry of hydraulic fractures. SPE/DOE low permeability symposium, Denver, Colorado. 27-29 May.

14. Siebrits, E., Peirce, A.P. (2002): An efficient multi-layer planar 3D fracture growth algorithm using a fixed mesh approach. *Int J Numer Meth Eng*. 53(3), 691-717.

15. Mack, M.G., Warpinski, N.R. (2000): Mechanics of hydraulic fracturing. In:Economides, Nolte, editors. Reservoir stimulation. 3rd ed. Chichester; Wiley.

16. Crosby, D.G., Rahman, M.M., Rahman, M.K., Rahman, S.S. (2002): Single and multiple transverse fracture initiation from horizontal wells. *Journal of Petroleum Science and Engineering.* 35(3-4), 191-204.

17. Ahmed, U., Strawn, J., Wilson, M. (1983): Effect of Stress Distribution on Hydraulic Fracture Geometry: A Laboratory Simulation Study in One Meter Cubic Blocks. SPE/DOE Low Permeability Gas Reservoirs Symposium, Denver, Colorado. 14-16 March.

18. Ketterij, R.G. van de., Pater, C.J. de. (1997): Experimental study on the impact of perforations on hydraulic fracturing tortuosity. SPE European Formation Damage Conference held in The Hague, The Netherlands. 2-3 June.

19. Deng, J.G., Guo, X.M., Sun, Y., Qi, B., Lei. W. (2008): Research on oriented perforation optimization technique for fracturing wells in tight gas reservoir. *Oil Drilling & Production Technology*. 30(6), 93-96.

20. Deng, J.G., Yu, B.H., Wang, J.F., Wang, B.Y., Li, B. (2003): Simulation Trial Research on Increasing Hydraulic Fracturing Efficiency of Low Permeability Reservoir by Oriented Perforation. Petroleum Drilling Techniques. 31(5), 14-16.

21. Pater, C.J. de., Cleary, M.P., Quinn, T.S., Barr, D.T., Johnson, D.E., Weijers L. (1994): Experimental verification of dimensional analysis for hydraulic fracturing. *SPE Production & Facilities*. 9(4), 230-238.

22. Pang, F. (1995): Model laws and tests on hydraulic fracturing. Shandong, Petroleum engineering, University of Petroleum, China.

23. Bunger, A.P., Jeffrey, R.G., Detournay, E. (2005): Application of scaling laws to laboratory-scale hydraulic fractures. Alaska Rocks 2005, The 40th U.S. Symposium on Rock Mechanics (USRMS), Anchorage, AK. 25-29 June.

24. Liu, G.H., Pang, F., Chen, Z.X. (2000): Development of scaling laws for hydraulic fracture simulation tests. *Journal of the University of Petroleum*, China (Edition of Natural Science). 24(5): 45-48.

25. Clitton, R.J., Abou-Sayed, A.S. (1979): On the computation of the three-dimensional geometry of hydraulic fractures. Symposium on Low Permeability Gas Reservoirs, Denver, Colorado. 20-22 May.

26. Zhou, J., Jin, Y., Chen, M. (2010): Experimental investigation of hydraulic fracturing in random naturally fractured blocks. *International Journal of Rock Mechanics & Mining Sciences.* 47(7), 1193-1199.

27. Brumley, J.L., Abass, H.H. (1996): Hydraulic Fracturing of Deviated Wells: Interpretation of Breakdown and Initial Fracture Opening Pressure. SPE Eastern Regional Meeting, Columbus, Ohio. 23-25 October.

28. Doe, T.W., Boyce, G. (1989): Orientation of Hydraulic Fractures in Salt Under Hydrostatic and Non-Hydrostatic Stresses. *Int J Rock Mech Min Sci & Geomech Abstr.* 26(6), 605-605.

29. Beach, A. (1980): Numerical Models of Hydraulic Fracturing and the Interpretation of Syntectonic Veins. J Str Geo. 2(4), 425.

30. Daneshy, A.A. (1974): Hydraulic Fracture Propagation in the Presence of Planes of Weakness. SPE European Spring Meeting, Amsterdam, Netherlands. 29-30 May.

31. Yew, C.H. (1997): Gulf Publishing Company, Houston, Texas. Mechanics of hydraulic fracturing.

32. Yew, C.H., Li, Y. (1987): Fracturing of a deviated well. *SPE Production Engineering.* 3(4), 429-437.

33. Soliman, M.Y., Boonen, Paul. (2000): Rock mechanics and stimulation aspects of horizontal wells. *Journal of Petroleum Science and Engineering.* 25(3-4), 187-204.

34. Soliman, M.Y., Lody, East., David, Adams. (2004): Geomechanics aspects of multiple fracturing of horizontal and vertical wells. SPE International Thermal Operations and Heavy Oil Symposium and Western Regional Meeting, Bakersfield, California. 16-18 March.

35. Hossain, M.M., Rahman, M.K., Rahman, S.S. (1999): A comprehensive monograph for hydraulic fracturing initiation from deviated wellbores under arbitrary stress regimes. SPE Asia Pacific Oil and Gas Conference and Exhibition, Jakarta, Indonesia. 20-22 April.

36. Hossain, M.M., Rahrnan, M.K., Rahman, S.S. (2000): Hydraulic fracture initiation and propagation: roles of wellbore trajectory, perforation and stress regimes. *J. Pet. Sci. & Eng.* 27(3-4), 129-149.

37. Crosby, D.G., Yang, Z., Rahman, S.S. (2001):

Methodology to predict the initiation of multiple transverse fractures from horizontal wellbores. *Journal of Canadian Petroleum Technology*. 40(10), 68-75.

38. Biao, F.J., Liu, H., Zhang, J. (2011): A numerical study of fracture initiation pressure under helical perforation conditions. *Journal of university of science and technology of China*. (41), 219-226.
39. Fallahzadeh, S.H., Shadizadeh, S.R., Pourafshary, P. (2010): Dealing with the challenges of hydraulic fracturing in deviated cased perforated boreholes. Trinidad and Tobago Energy Resources Conference, Port of Spain, Trinidad. 27-30 June.
40. Fallahzadeh, S.H., Shadizadeh, S.R., Pourafshary, P., Zare, M.R. (2010): Modelling the perforation stress profile for analyzing hydraulic fracturing initiation in a cased Hole. Nigeria Annual International Conference and Exhibition, Tinapa - Calabar, Nigeria. 31 July-7 August.
41. Ketterij, R.G. van de, Pater, C.J. de. (1999): Impact of perforations on hydraulic fracturing *Tortuosity. SPE Prod. & Facilities*. 14(2), 131-138.
42. Weng, X.W. (1993): Fracture initiation and propagation from deviated wellbores. SPE Annual Technical Conference and Exhibition, Houston, Texas. 3-6 October.
43. Luo, T.Y., Guo, J.C., Zhao, J.Z., Wang, J.H., Pan, J.J. (2007): Study on fracture initiation pressure and fracture starting point in deviated wellbore with perforations. *ACTA PETROL EI SINICA*. 28(1), 139-142.
44. Chen, M., Chen, Z.X., Huang, R.Z. (1995): Hydraulic fracturing of highly deviated wells. *Journal of the University of Petroleum, China*. 19(2), 30-35.
45. Deng, J.G., Wang, J.F., Yan, J.H. (2002): Study on propagation law of hydraulic fracturings of gas pool in unconsolidated sandstone. *Rock and Soil Mechanics*. 23(1), 72-74.
46. Osorio, J.G., Lopez, C.F. (2009): Geomechanical Factors Affecting the hydraulic fracturing performance in a geomechanically complex, tectonically active area in colombia. Latin American and Caribbean Petroleum Engineering Conference, Cartagena de Indias, Colombia. 31 May-3 June.
47. Stadulis, L.M. (1995): Development of completion design to screenouts caused by multiple near wellbore fractures. Low Permeability Reservoirs Symposium, Denver, Colorado. 19-22 March.
48. Kim, C.M., Abass, H.H. (1991): Hydraulic fracture initiation from horizontal wellbores: Laboratory experiments. The 32nd U.S. Symposium on Rock Mechanics (USRMS), Norman, Oklahoma. 10-12 July.